The High Efficiency fast-Response GAmma (HERGA) detector based on SiPM readout

C. Altomare[1], D. Cerasole[1,2], L. Di Venere[1]*, E. Fanchini[3], F. Gargano[1], F. Giordano[1,2], F. Loparco[1,2], S. Loporchio[1,2], A. Mastroserio[1,4], M. Morichi[3], F. R. Pantaleo[1,2], D. Serini[1], P. Spinelli[1,2], L. Swiderski[5]

[1]Istituto Nazionale di Fisica Nucleare - Sezione di Bari, Italy
[2]Dipartimento Interateneo di Fisica dell'Università e del Politecnico di Bari, Italy
[3]CAEN s.p.a. - Viareggio, Italy
[4]Università di Foggia
[5]National Centre for Nuclear Research (NCBJ), 05-400 Otwock-Swierk, Poland
(*) leonardo.divenere@ba.infn.it

***Abstract*—Gamma-ray spectroscopy and gamma-ray imaging are two complementary techniques used for the localization and the identification of radioactive sources containing gamma-ray emitting radioisotopes. The radioactivity monitoring is focused on the detection of both artificial and environmental radioactive sources like Naturally Occurring Radioactive Materials (NORM). This kind of contamination becomes dangerous when the detection of the unwanted substances exhibits a concentration significantly above the environmental radioactive background radiation levels. For this purpose, we have developed, tested and shown a High Efficiency fast-Response GAmma (HERGA) detector useful for the identification of radionuclides and for gamma-ray imaging. A first version of the gamma detector prototype was composed of 16 CsI(Tl) scintillating crystals of 3x3x10 cm3 size, arranged in 4x4 matrix coupled with standard Photomultiplier tubes (PMTs). An image reconstruction of a radioactive gamma emitter source is possible using the coded mask technique, in which a 7x7 mask, made of Plastic and Tungsten tiles, is placed in front of the detector and a pattern recognition algorithm based on classical statistical methods (Kolmogorov Smirnov) is used to reconstruct the source position. The measurements carried out showed a point spread function (PSF) of a few mrad for pointlike sources. The Minimum Detectable Activity (MDA) was also determined in the case of pointlike radioactive sources. In this contribution we will present an update of the HERGA detector prototype in which Silicon Photomultipliers (SiPMs) are used in place of the PMTs. SiPMs provide similar or even better performance compared to the standard PMT sand provide benefits in terms of lower power consumption and reduced cost and compactness. The advantages of the SiPM technology are also characterized by the robustness of the photosensor that makes the new prototype compact, portable, ideal for in-situ and real-time. We will show a comparison between the results obtained with the newest SiPM read-out technology with respect to those obtained with the PMT one, in terms of energy and spatial resolution. The imaging performance is also in phase of testing in order to localize extended radioactive sources such as for example NORM samples or to detect inaccessible or hidden nuclear waste.**

***Keywords* —Gamma rays, environmental monitoring, NORM, scintillator crystals, Silicon Photomultipliers.**

I. Introduction

THE detection of gamma rays of ambient origin is of very wide interest in several fields, such as the homeland security, environmental monitoring, detection of illegal radioisotopes trades, in medical science. The radioactivity monitoring is focused on the detection of both artificial and environmental radioactive sources. The latter include Naturally Occurring Radioactive Materials (NORM), which are materials containing any of the primordial radionuclides or radioactive elements as they occur in nature, such as radium, uranium, thorium, potassium and their radioactive decay products, such as radon [1]. This kind of contamination is dangerous when the presence of unwanted substances exhibits a concentration significantly above the environmental radioactive background radiation levels [2].

Gamma-ray spectroscopy and imaging are widely used and combined to identify and localize sources containing gamma-ray emitting radioisotopes, respectively. Gamma-ray spectroscopy is based on the measurement of the gamma-ray energy, allowing the identification of the radionuclide through its characteristic emission lines. In addition, imaging techniques can be used to measure the radioactive source position. Different techniques can be employed to reconstruct the gamma-ray directions. Among these, the coded mask technique is widely used especially in astrophysics and medical to precisely localize X-rays and gamma rays with energy from tens of keV to few MeV [3].

The scintillator technology is nowadays widely being adopted for environmental monitoring. Thanks to their high Z number, inorganic scintillators guarantee a high efficiency in the gamma-ray detection. They are usually equipped with traditional photomultiplier tubes (PMTs) or modern photon detectors like Silicon Photomultipliers (SiPMs) to detect the scintillation light and measure the gamma ray energy. An

extensive review is collected in [4].

II. THE HERGA PROTOTYPE

In this work, we present a gamma-ray detector prototype with high efficiency and source localization capabilities based on the coded mask technique, named High Efficiency fast-Response GAmma detector (HERGA). A full description and characterization of this detector is presented in [5].

The HERGA prototype is composed of an array of 4 × 4 CsI(Tl) scintillator crystals (3 × 3 × 10 cm^3), each coupled to a PMT (ET Enterprises, 9124B, 26% quantum efficiency at 400 nm) with a Cockcroft–Walton voltage multiplier as high voltage supplier (ET Enterprises, electron tubes, HV3020CN). The total weight of the detector is ~ 8 kg. The readout system is based on a CAEN V1725 16-channel digitizer (14-bit ADC and 250 MS/s sampling frequency), which is used to generate the trigger and digitize the PMT signals. The 16 signals from the 16 PMTs are recorded and integrated with an on-line custom analysis software providing count spectra in real time. A coded mask, consisting of an array of 7 × 7 PVC and tungsten tiles, which are respectively transparent and opaque to gamma rays, is placed in front of the detector. The mask is generated from a 4 × 4 Modified Uniform Redundant Array (MURA). Its throughput, defined as the fraction of transparent pixels, is equal to 38.8%. Each tile has a size of 3 × 3 × 1 cm^3, while the whole mask has a size of 21 × 21 × 1 cm^3 and a weight of ~ 6 kg. FIGURE 1 shows a picture of the detector prototype.

The image reconstruction performances of the detector were studied with Monte Carlo simulations based on Geant4 and tested experimentally in laboratory with radioactive sources.

Fig. 1. Picture of the HERGA prototype.

A. Data acquisition and Energy calibration

Signals from the 16 CsI(Tl) scintillator crystals each one coupled to one PMT were acquired with the V1725 digitizer. Several radioactive sources were used to measure the PMT signals as a function of energy. The gamma detector was operated in self-triggering mode. A trigger was generated whenever the pulse height from any PMT exceeded a preset threshold value, which could be adjusted for individual channels. When a trigger occurred, the pulses from all PMTs were integrated and the charge values were recorded by the digitizer. The gains of the 16 PMTs and the thresholds were adjusted to equalize the individual trigger rates. The signal integration time was optimized to maximize the energy resolution and fixed to 2 μs.

The energy calibration was performed using eight radioactive sources placed at 15 cm from the detector. The gamma-ray energy spectra were fitted with Gaussian functions to describe the gamma-ray peaks and a second order polynomial function describing the background. The peak positions allow to determine the calibration functions, while the peak widths provide a measurement of the energy resolution.

Fig. 2 shows the calibration curve of one of the crystals, which exhibits a good linearity up to 1500 keV, and its energy resolution $\sigma(E)/E$. The energy resolution curve in FIGURE was well described with the function $\sigma(E)/E \approx 4.1\%/\sqrt{E(MeV)}$. A similar behavior is observed for all scintillator bars.

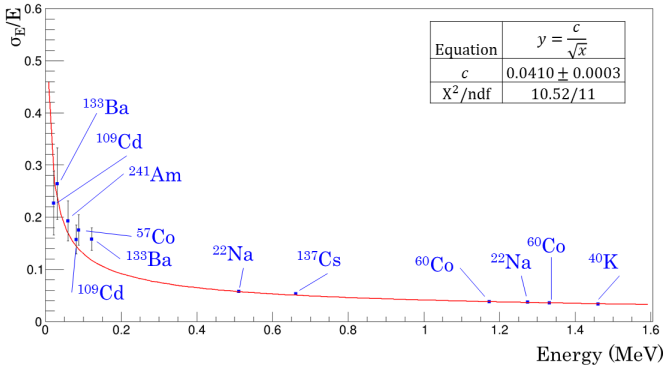

Fig. 2. Energy resolution curve for one the scintillator crystals.

B. Position reconstruction and angular resolution.

The HERGA prototype has capabilities to reconstruct the position of the gamma ray sources exploiting the coded mask technique. A Monte Carlo simulation based on GEANT4 (REF) was built to study the performance of the detector and to validate the reconstruction algorithm. Gamma rays were generated from a point-like source with isotropic emission characterized by an energy value extracted from the radioisotope energy peak distribution. The source was placed at a fixed distance z = 40 cm from the detector and its position was changed on a plane parallel to the detector surface. The mask was placed between the detector and the source, at z = 10 cm from the detector and at 30 cm from the source. In each simulation the 16 count spectra corresponding to each scintillator crystal were recorded. Three radioactive sources were used to test the reconstruction capabilities as a function of the gamma-ray energy, namely ^{60}Co, ^{137}Cs and ^{241}Am.

The reconstruction method was based on a two dimensional Kolmogorov-Smirnov test. At first, simulations were performed varying the radioactive source position. For each simulation, the image produced in the scintillator array by the radioactive source was recorded and a database of these images was built. The reconstruction of the position of an unknown

source was then performed defining a similarity probability of the unknown image with the database. The weighted average position provides the optimal reconstructed position.

The theoretical resolution of the detector is estimated performing a great number of simulation runs. Fig. 3(a) shows the 2D distribution of the reconstructed positions when a source of ^{60}Co is placed in the central position. The angular separation between the reconstructed and simulated positions was then calculated for each simulation. Its distribution is shown in Fig. 3(b) and the 68% and 95% quantiles were calculated and provide an estimate of the Point Spread Function (PSF) of the instrument. Fig. 4 shows the 68% and 95% quantiles of the PSF evaluated simulating a ^{60}Co, a ^{137}Cs and an ^{241}Am source at different positions along the diagonal of the detector plane. We note that the angular resolution deteriorates as the gamma-ray energy increases, since the absorption efficiency of the tungsten pixels in the mask decreases with increasing photon energy.

The angular resolution was measured experimentally using the same radioactive sources. A database of images was built by placing the radioactive sources on a grid with a 1-cm step. The reconstruction algorithm was then tested with a source placed at the center of the detector and at a distance of 3 cm along the x- and y- axis from the center. A PSF of 4±2.5 mrad was measured for a 60Co source placed in the central position, in agreement with the Monte Carlo simulation predictions.

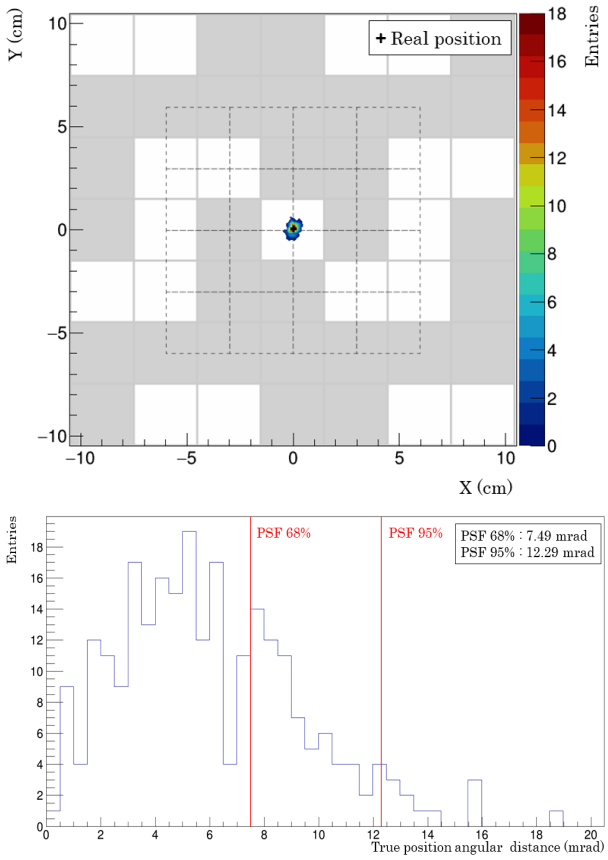

Fig. 3. (a) Two dimensional reconstructed positions for a simulated 60Co source placed at the center of the detector. (b) Angular separation between the simulated and reconstructed positions. The red lines show the 68% and 95% quantiles of the distribution.

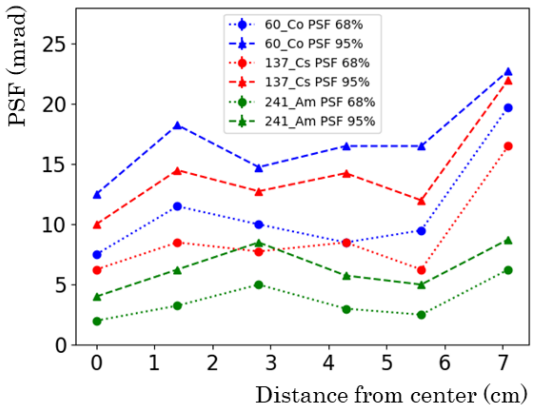

Fig. 4. 68% and 95% PSFs for three radioactive sources placed in different positions along the diagonal of the detector plane.

C. *Minimum Detectable Activity*

Finally, the minimum detectable activity (MDA) of the detector was measured. The gamma camera was placed in a 5 cm thick lead shield to reduce the environmental background. The radioactive sources were placed on the front face of the camera. The coded mask was removed to maximize the radiation throughput. Six different radioactive sources were placed at a distance of 15 cm from the detector and their spectra were measured by varying the acquisition time in the range from 15 to 120 min with 15- min steps.

To evaluate the MDA, the efficiency calibration is required, which was measured with sources with known activities: ^{241}Am, ^{57}Co, ^{137}Cs, ^{60}Co, ^{152}Eu and ^{22}Na. The spectra were analyzed with the Quantus - Quantitative Spectrometry Software by CAEN and the efficiency ϵ was calculated as the ratio between the number of detected photons and the number of emitted photons. The efficiency curve $\epsilon(E)$ was fitted with the following function:

$$\ln(\epsilon(E)) = \sum_k a_k \left(\frac{E}{E_0}\right)^k$$

where E_0 = 1 keV is a fixed scale energy. Fig. 5 shows the measured points and the best fit curve.

Finally, the MDA was measured as a function of the acquisition time using the following equation:

$$MDA(Bq) = \frac{L_D}{t_m(s) \times \epsilon \times b}$$

where t_m is the source acquisition time, b is the relative line intensity for the specific gamma-ray emission peak, which corresponds to the probability of a gamma-ray emission with the line energy in a radioactive decay event, ϵ is the calculated efficiency for the specific peak, L_D is the critical level of counts above the background to detect a source, that is given by [6]:

$$L_D = 4.65 \times \sqrt{R_b(s^{-1}) \times t_m(s)} + 3$$

where R_b is the background count rate.

Fig. 6 shows the MDA for ^{137}Cs source for data acquisition times from 15 to 120 min. The values of the MDA have been fitted with a power-law function $MDA = c\, t^a$, where t is the

acquisition time. We see that the MDA is roughly proportional to the inverse of the square root of the acquisition time, as expected.

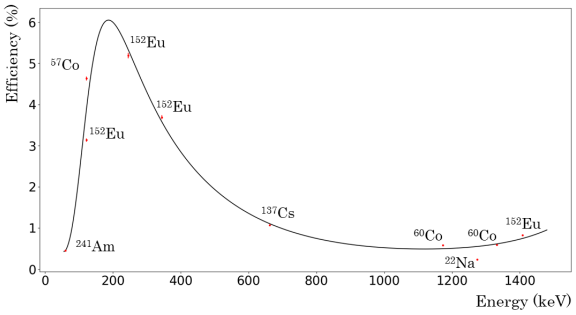

Fig. 5. Efficiency curve for the HERGA prototype measured for the MDA calculation.

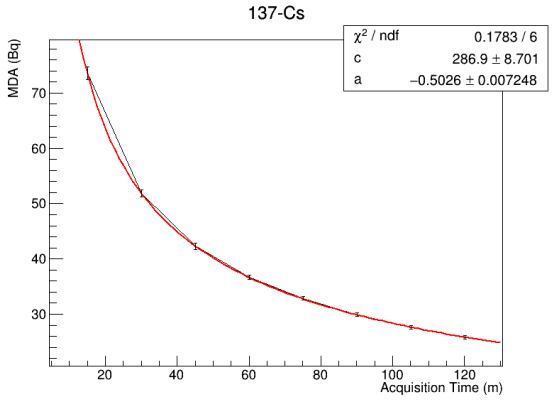

Fig. 6. MDA as a function of the acquisition time for a ^{137}Cs source

III. The HERGA upgrade

The HERGA prototype proved to have excellent performance in terms of angular resolution and MDA. An upgrade of the detector is foreseen to make the instrument more compact and portable. The first step is the employment of SiPMs in place of the PMTs. This reduces the overall volume and weight of the instrument, still keeping its performances. A prototype crystal was built employing 6x6 mm^2 SiPMs (Hamamatsu S14160-6050HS) mounted on custom PCBs. Two SiPMs were connected in parallel on the small face of a 3x3x10 cm^3 CsI(Tl) crystal in order to detect enough scintillation light and increase the energy resolution. A picture of the prototype is shown in Fig. 7. The energy resolution of this prototype was measured with ^{241}Am, ^{137}Cs and ^{60}Co radioactive sources. Results are reported in Table I and are comparable with the ones obtained with the PMT prototype and shown in previous section.

TABLE I
ENERGY RESOLUTION FOR SIPM PROTOTYPE

Radioisotope	Energy (keV)	Resolution
^{241}Am	59.5	29%
^{137}Cs	661.7	10%
^{60}Co	1173	6%
^{60}Co	1332	7%

Fig. 7. CsI(Tl) crystal coupled to Hamamatsu S14160-6050HS SiPMs

IV. Future perspectives

In this work a gamma-ray detector with imaging capability was developed, based on a CsI(Tl) crystal array coupled to PMTs. A coded mask reconstruction technique was employed to reconstruct the gamma-ray source position, reaching a PSF at the level of few mrad. In addition, the large active volume of the prototype also resulted in a very low MDA. An upgrade of this prototype is foreseen based on SiPMs and a compact and low power electronics, in order to make the instrument compact and portable. A preliminary prototype was built based on 4 CsI(Tl) crystals and used for the first in-situ measurements on the Nisyros Island in Greece. Data analysis is ongoing and will be presented in a future work.

References

[1] S. Chaki, E. Foutes, S. Ghose, B. Littleton, J. Mackinney, D. Schultheisz, M. Schuknecht, L. Setlow, B. Shroff, T. Peake, Technical Report on Technologically Enhanced Naturally Occurring Radioactive Materials from Uranium Mining Volume 1: Mining and Reclamation Background, Citeseer, 2008, URL http://citeseerx.ist.psu.edu/viewdoc/summary?doi=10.1.1.348.3026 .W.-K. Chen, Linear Networks and Systems. Belmont, CA, USA: Wadsworth, 1993, pp. 123–135.

[2] P.M. Chapman, Determining when contamination is pollution—weight of evidence determinations for sediments and effluents, Environ. Int. 33 (4) (2007) 492–501, URL: https://www.sciencedirect.com/science/article/pii/S0160412006000136X.

[3] H. Anger, A new instrument for mapping gamma-ray emitters, Biol. Med. Quarterly Rep. UCRL 3653 (1957) 38.

[4] H. Al Hamrashdi, D. Cheneler, S.D. Monk, A fast and portable imager for neutron and gamma emitting radionuclides, Nucl. Instrum. Methods Phys. Res. A 953 (2020) 163253, URL https://www.sciencedirect.com/science/article/pii/S0168900219315256.

[5] C. Altomare, L. Di Venere, F.R. Pantaleo, E. Fanchini, F. Giordano, F. Loparco, M. Morichi, P. Spinelli, L. Swiderski, A high efficiency fast-response gamma detector with mrad pointing capabilities, Nuclear Inst. and Methods in Physics Research, A 1025 (2022) 166106

[6] L.A. Currie, Limits for qualitative detection and quantitative determination. application to radiochemistry, Anal. Chem. 40 (3) (1968) 586–593, URL https://pubs.acs.org/doi/pdf/10.1021/ac60259a007